Measurement of CP violation and mixing in $B_s^0 \to J/\psi\phi$ in ATLAS

QCD 2019
Montpellier, France
05. 07. 2019

Tomas Jakoubek
on behalf of the ATLAS Collaboration
Czech Academy of Sciences | tomas.jakoubek@cern.ch

Introduction

- Decay $B_s^0 \to J/\psi\phi$ is expected to be sensitive to new physics contributions to CP violation.
- Neutral B_s^0 meson can oscillate into its antiparticle $\overline{B_s^0}$ (and vice versa).
- The oscillation frequency is characterized by the mass difference Δm_s of the heavy (B_H) and light (B_L) mass eigenstates.
- In the absence of CP violation, the B_H state would correspond to the CP-odd state and the B_L to the CP-even state.

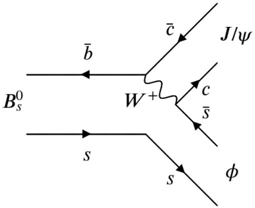

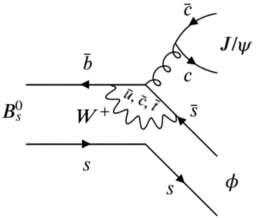

Types of CP Violation

- CP **violation in decay** (or direct CP violation): decay amplitudes of mesons $M \to f$ and $\overline{M} \to \overline{f}$ are different.
- CP **violation in mixing** (or indirect CP violation): asymmetry in the particle antiparticle oscillations... In this case the CP eigenstates are not equivalent to the mass eigenstates.
- CP **violation in interference of mixing and decay** can only occur if M^0 and $\overline{M^0}$ decay into the same final state;
  The common final state is reached via two different decay chains:
  $M^0 \to f$ and $M^0 \to \overline{M^0} \to f$ (case of $B_s^0 \to J/\psi\phi$).

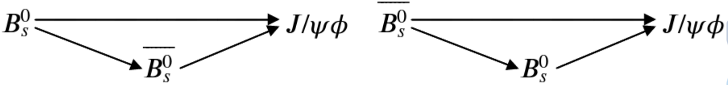

Motivation: New Physics

- *CP* violating phase is defined as the weak phase difference between the $B_s^0 - \overline{B_s^0}$ mixing amplitude and the $b \to c\bar{c}s$ decay amplitude.
- In the Standard Model (SM) it can be related to the CKM matrix [1]

$$\phi_s \simeq -2\beta_s = -2\arg\left(-\frac{V_{ts}V_{tb}^*}{V_{cs}V_{cb}^*}\right). \tag{1}$$

  and then $\phi_s = -0.0363^{+0.0016}_{-0.0015}$ rad can be predicted [2].
- Any sizeable deviation from this value would be a sign of beyond SM physics.
- The New Physics processes could introduce additional contributions to the box diagrams describing the $B_s^0 - \overline{B_s^0}$ mixing.

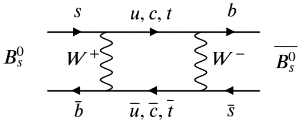

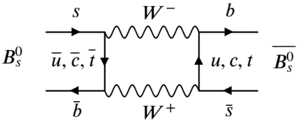

The ATLAS Experiment

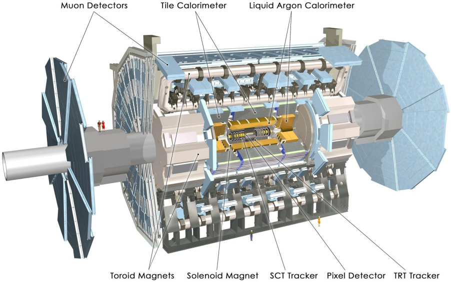

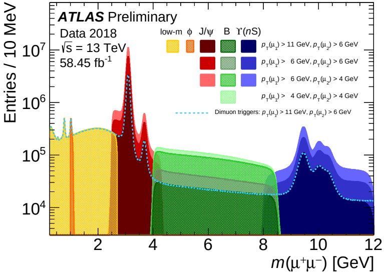

- **Muon Spectrometer:** triggering $|\eta| < 2.4$ and precision tracking $|\eta| < 2.7$.
- **Inner Detector:** Silicon Pixels and Strips with Transition Radiation Tracker, $p_T > 0.4$ GeV and $|\eta| < 2.5$,
  - **NEW in Run2:** "Insertable B-Layer" (IBL) - additional inner-most pixel layer (r = 33 mm) and lower x/X_0 beam pipe,
  - **resolution in $m(\mu^+\mu^-)$:** Around 50 MeV at J/ψ, 150 MeV at $\Upsilon(nS)$,
  - **resolution in b-hadron proper decay time:** ~100 fs (30 % improvement with IBL).

Used Data

- 4.9 fb^{-1} 7 TeV *pp* 2011 (untagged [5] + tagged [6]).
- 14.3 fb^{-1} 8 TeV *pp* 2012 (statistically combined with 7 TeV to full Run1 tagged analysis [7]).
- **NEW:** 80.5 fb^{-1} 13 TeV *pp* 2015-2017 (stat. comb. with Run1 [8]).
- Collected by trigger based on identification of $J/\psi \to \mu^+\mu^-$ with $p_{\text{T}}(\mu)$ threshold (vary over run periods).
- Two muon tracks and two tracks (no PID, but not muons), refitting, using only the best candidate in the event.
- No lifetime cut! Signal-background separation done by the fit.

Angular Analysis

- $B_s^0 \to J/\psi\phi$ = pseudoscalar to vector-vector final state $\to$ admixture of CP-odd ($L = 1$) and CP-even ($L = 0, 2$) states.
- Distinguishable through time-dependent angular analysis.
- Non-resonant S-wave decay $B_s^0 \to J/\psi K^+K^-$ and $B_s^0 \to J/\psi f_0$ both contribute to the final state:
  - cannot be identified in the measured data,
  - can significantly bias measurement of ϕ_s,
  - included in the differential decay rate due to interference with the signal decay.

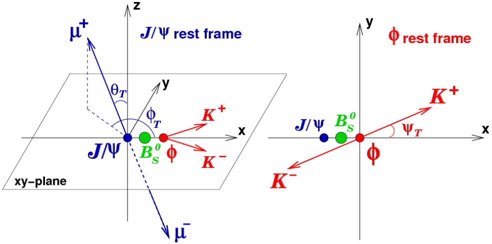

Flavour Tagging

- Knowledge of the initial flavour can improve any *CP* violation measurement.
- At the LHC *B*-mesons are produced in the hadronization of $b\bar{b}$ pair.
- The majority of these pairs are produced either both in the forward or both in the backward direction of the detector.
- Self-tagging $B^{\pm} \to J/\psi K^{\pm}$ channel used for calibration and performance estimation.

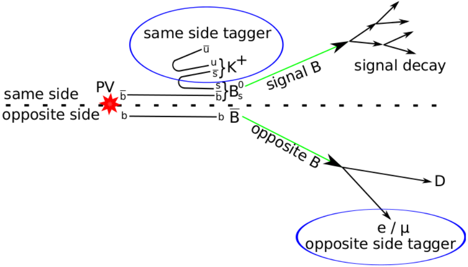

Flavour Tagging

Opposite Side Tagging Methods

Muon/electron tagging: semi-leptonic decay of B ($b \to \mu/e$ transition),

- flavour given by lepton charge,
- diluted by $b \to c \to \ell$ cascade decays and neutral B-meson oscillations,
- improved by using momentum weighed charge of lepton and tracks around the leading lepton

$$Q_\ell = \frac{\sum_i^{N_{\text{tracks}}} q_i\, p_{\text{T}i}^{\kappa}}{\sum_i^{N_{\text{tracks}}} p_{\text{T}i}^{\kappa}}, \qquad (2)$$

where N_{tracks} is number of tracks in the cone $\Delta R < 0.5$ around the leading lepton, q_i and $p_{\text{T}i}$ are charge and p_{T} of the track, respectively, and the constant $\kappa = 1.1$ (found empirically).

b-jet-charge tagging: used if the additional muon/electron is absent; momentum-weighted track-charge in jet.

Flavour Tagging
Calibration Curves

- From a calibration sample, the opposite-side charge is mapped to a probability that the event is B_s^0 (or $\overline{B_s^0}$), and put into the likelihood fit on per-candidate basis.
- If there is no tagging information, $P = 0.5$ is assigned.

Tag method	Efficiency [%]	Effective Dilution [%]	Tagging Power [%]
Tight muon	4.50 ± 0.01	43.8 ± 0.2	0.862 ± 0.009
Electron	1.57 ± 0.01	41.8 ± 0.2	0.274 ± 0.004
Low-p_T muon	3.12 ± 0.01	29.9 ± 0.2	0.278 ± 0.006
Jet	5.54 ± 0.01	20.4 ± 0.1	0.231 ± 0.005
Total	14.74 ± 0.02	33.4 ± 0.1	1.65 ± 0.01

$$\epsilon_{\text{tag}} = \frac{N_{\text{tagged}}}{N_{\text{total}}}, \quad (3)$$

$$\mathcal{D}_{\text{tag}} = 1 - \frac{2\,N_{\text{wrong}}}{N_{\text{tagged}}}, \quad (4)$$

$$P_{\text{tag}} = \epsilon_{\text{tag}} \cdot \mathcal{D}^2_{\text{tag}}. \quad (5)$$

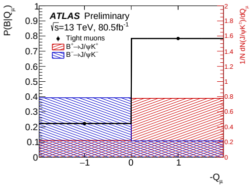

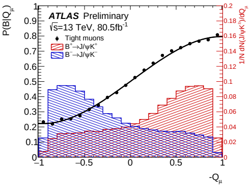

Maximum Likelihood Fit

Variables

- Observed variables:
  - B_s^0 mass m_i and its uncertainty σ_{m_i},
  - B_s^0 proper decay time t_i and its uncertainty σ_{t_i}; $t = \frac{L_{xy} m_B}{p_{\mathrm{T}}}$,
  - 3 angles between final state particles in transversity basis $\Omega_i(\theta_{Ti}, \phi_{Ti}, \psi_{Ti})$,
  - B_s^0 momentum $p_{\mathrm{T}i}$,
  - B_s^0 tag probability $P(B|Q_i)$ and tagging method M_i.
- Determine 9 physics variables to describe $B_s^0 \to J/\psi\phi$ and S-wave: $\phi_s, \Delta\Gamma_s, \Gamma_s, |A_0(0)|^2, |A_{||}(0)|^2, |A_S(0)|^2, \delta_{||}, \delta_{\perp}, \delta_S$.
- Likelihood function:

$$\ln \mathcal{L} = \sum_{i=1}^{N} \left\{ w_i \cdot \ln \left(f_{\mathrm{sig}} \cdot \mathcal{F}_{\mathrm{sig}} + f_{\mathrm{sig}} \cdot f_{B_d^0} \cdot \mathcal{F}_{B_d^0} + f_{\mathrm{sig}} \cdot f_{\Lambda_b} \cdot \mathcal{F}_{\Lambda_b} + (1 - f_{\mathrm{sig}}(1 + f_{B_d^0} + f_{\Lambda_b})) \cdot \mathcal{F}_{\mathrm{bck}} \right) \right\}.$$

Maximum Likelihood Fit
Probability Density Functions (PDF)

- Signal PDF consists of:
  - **mass PDF**: Gaussian with per-candidate width and scale-factor,
  - **time-angular PDF** convolved with time resolution function $G(t_i, \sigma_{t_i})$; flavour-dependent terms weighted by the corresponding tagging probability,
  - 4D angular **acceptance** (in bins of p_T, from MC),
  - empirical distributions of (conditional) observables σ_{m_i}, σ_{t_i}, $p_{T\,i}$, and $P(B|Q)$
- Background PDF:
  - **mass PDF**: exponential + constant term,
  - **time PDF**: δ-function + 3 exponentials convolved with $G(t_i, \sigma_{t_i})$,
  - **angular PDF**: Legendre polynomial functions.

- Fit projection to all data passing selections (3 210 429 B_s^0 candidates).
- Pull plots include both stat. and syst. uncertainties.
- Deviations within 2σ and thus covered by declared systematics.

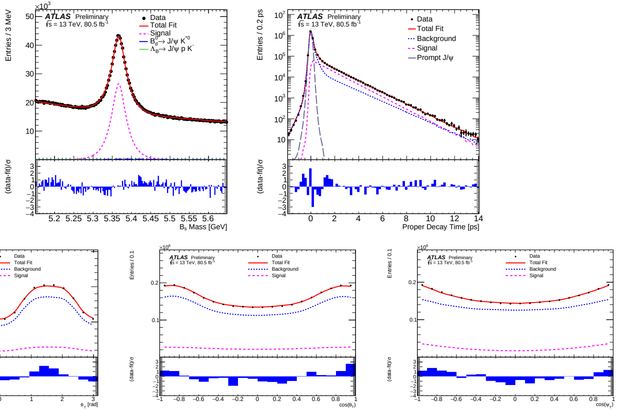

Results

Combination Run1 + Data 2015-2017

- Ambiguity in sign of $\Delta\Gamma_s$:

$$\{\phi_s, \Delta\Gamma_s, \delta_\perp, \delta_\parallel\} \rightarrow \{\pi - \phi_s, -\Delta\Gamma_s, \pi - \delta_\perp, 2\pi - \delta_\parallel\}, \tag{6}$$

  $\Delta\Gamma_s > 0$ constrained by LHC*b* [11].
- The combination makes use of a Best Linear Unbiased Estimate (BLUE) method [12, 13].

Parameter	Run1 Data			13 TeV Data			Combined		
	Value	Stat.	Syst.	Value	Stat.	Syst.	Value	Stat.	Syst.
ϕ_s [rad]	-0.090	0.078	0.041	-0.068	0.038	0.018	-0.076	0.034	0.019
$\Delta\Gamma_s$ [ps^{-1}]	0.085	0.011	0.007	0.067	0.005	0.002	0.068	0.004	0.003
Γ_s [ps^{-1}]	0.675	0.003	0.003	0.669	0.001	0.001	0.669	0.001	0.001
$\|A_0(0)\|^2$	0.522	0.003	0.007	0.517	0.001	0.004	0.517	0.001	0.004
$\|A_\parallel(0)\|^2$	0.227	0.004	0.006	0.219	0.002	0.002	0.220	0.002	0.002
$\|A_S(0)\|^2$	0.072	0.007	0.018	0.046	0.003	0.004	0.043	0.004	0.004
$\delta_\perp$ [rad]	4.15	0.32	0.16	2.946	0.101	0.097	3.075	0.096	0.091
$\delta_\parallel$ [rad]	3.15	0.10	0.05	3.267	0.082	0.201	3.295	0.079	0.202
$\delta_\perp - \delta_S$ [rad]	-0.08	0.03	0.01	-0.220	0.037	0.010	-0.216	0.037	0.010

Results
Combination Run1 + Data 2015-2017

- Ambiguity in sign of $\Delta\Gamma_s$:

$$\{\phi_s, \Delta\Gamma_s, \delta_\perp, \delta_\parallel\} \rightarrow \{\pi - \phi_s, -\Delta\Gamma_s, \pi - \delta_\perp, 2\pi - \delta_\parallel\}, \tag{6}$$

  $\Delta\Gamma_s > 0$ constrained by LHC*b* [11].
- The combination makes use of a Best Linear Unbiased Estimate (BLUE) method [12, 13].

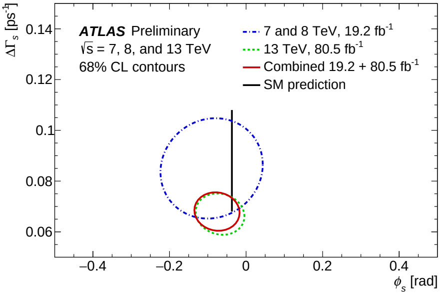

Comparison of the Results
(also Before vs. After)

	ϕ_s [rad]	$\Delta\Gamma_s\,[\mathrm{ps}^{-1}]$	Ref.
CMS	$-0.075 \pm 0.097 \pm 0.031$	$0.095 \pm 0.013 \pm 0.007$	[14]
LHC*b*	-0.041 ± 0.025	0.0816 ± 0.0048	many channels, [15]
ATLAS	$-0.076 \pm 0.034 \pm 0.019$	$0.068 \pm 0.004 \pm 0.003$	[8]
Comb.	-0.055 ± 0.021	$0.0764^{+0.0034}_{-0.0033}$	HFLAV Preliminary [16]
SM	$-0.0363^{+0.0016}_{-0.0015}$	0.087 ± 0.021	[2], [17], resp.

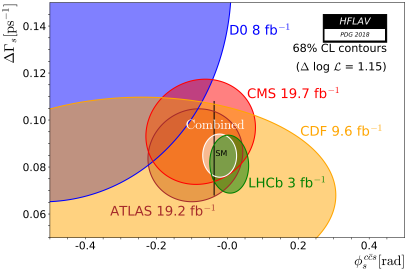

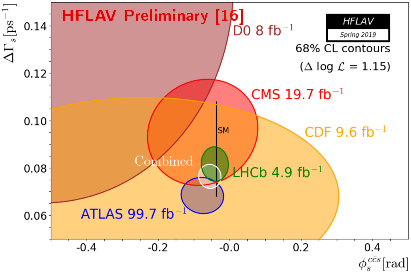

Summary

- **ATLAS** has produced very **impressive** and **competitive** results.
- Analysis of the 2015+2016+2017 ATLAS data of 80.5 fb^{-1} performed.
- Results combined with those from the previous Run1 analysis.
- Compatible with LHC*b* and CMS as well as with the SM prediction.
- Our new measurement improves precision of the parameters.
- Analysis of full Run2 (60 fb^{-1} more) ongoing.
- **More** public results on **ATLAS B-physics** TWiki page https://twiki.cern.ch/twiki/bin/view/AtlasPublic/BPhysPublicResults !

THANK YOU!

BACKUP

Decay Rate

- Ignoring detector effects, the distribution for the time and angles is given by the differential decay rate

$$\frac{\mathrm{d}^4\Gamma}{\mathrm{d}t\ \mathrm{d}\Omega} = \sum_{k=1}^{10} \mathcal{O}^{(k)}(t) g^{(k)}(\theta_T, \psi_T, \phi_T). \tag{7}$$

k	$\mathcal{O}^{(k)}(t)$	$g^{(k)}(\theta_T, \psi_T, \phi_T)$
1	$\frac{1}{2}\lvert A_0(0)\rvert^2 \left[(1+\cos\phi_s)\, e^{-\Gamma_\mathrm{L}^{(s)}t} + (1-\cos\phi_s)\, e^{-\Gamma_\mathrm{H}^{(s)}t} \pm 2e^{-\Gamma_s t}\sin(\Delta m_s t)\sin\phi_s\right]$	$2\cos^2\psi_T(1-\sin^2\theta_T\cos^2\phi_T)$
2	$\frac{1}{2}\lvert A_\parallel(0)\rvert^2 \left[(1+\cos\phi_s)\, e^{-\Gamma_\mathrm{L}^{(s)}t} + (1-\cos\phi_s)\, e^{-\Gamma_\mathrm{H}^{(s)}t} \pm 2e^{-\Gamma_s t}\sin(\Delta m_s t)\sin\phi_s\right]$	$\sin^2\psi_T(1-\sin^2\theta_T\sin^2\phi_T)$
3	$\frac{1}{2}\lvert A_\perp(0)\rvert^2 \left[(1-\cos\phi_s)\, e^{-\Gamma_\mathrm{L}^{(s)}t} + (1+\cos\phi_s)\, e^{-\Gamma_\mathrm{H}^{(s)}t} \mp 2e^{-\Gamma_s t}\sin(\Delta m_s t)\sin\phi_s\right]$	$\sin^2\psi_T\sin^2\theta_T$
4	$\frac{1}{2}\lvert A_0(0)\rvert\lvert A_\parallel(0)\rvert\cos\delta_\parallel \left[(1+\cos\phi_s)\, e^{-\Gamma_\mathrm{L}^{(s)}t} + (1-\cos\phi_s)\, e^{-\Gamma_\mathrm{H}^{(s)}t} \pm 2e^{-\Gamma_s t}\sin(\Delta m_s t)\sin\phi_s\right]$	$-\frac{1}{\sqrt{2}}\sin 2\psi_T\sin^2\theta_T\sin 2\phi_T$
5	$\lvert A_\parallel(0)\rvert\lvert A_\perp(0)\rvert[\frac{1}{2}(e^{-\Gamma_\mathrm{L}^{(s)}t} - e^{-\Gamma_\mathrm{H}^{(s)}t})\cos(\delta_\perp-\delta_\parallel)\sin\phi_s \pm e^{-\Gamma_s t}(\sin(\delta_\perp-\delta_\parallel)\cos(\Delta m_s t) - \cos(\delta_\perp-\delta_\parallel)\cos\phi_s\sin(\Delta m_s t))]$	$\sin^2\psi_T\sin 2\theta_T\sin\phi_T$
6	$\lvert A_0(0)\rvert\lvert A_\perp(0)\rvert[\frac{1}{2}(e^{-\Gamma_\mathrm{L}^{(s)}t} - e^{-\Gamma_\mathrm{H}^{(s)}t})\cos\delta_\perp\sin\phi_s \pm e^{-\Gamma_s t}(\sin\delta_\perp\cos(\Delta m_s t) - \cos\delta_\perp\cos\phi_s\sin(\Delta m_s t))]$	$\frac{1}{\sqrt{2}}\sin 2\psi_T\sin 2\theta_T\cos\phi_T$
7	$\frac{1}{2}\lvert A_S(0)\rvert^2 \left[(1-\cos\phi_s)\, e^{-\Gamma_\mathrm{L}^{(s)}t} + (1+\cos\phi_s)\, e^{-\Gamma_\mathrm{H}^{(s)}t} \mp 2e^{-\Gamma_s t}\sin(\Delta m_s t)\sin\phi_s\right]$	$\frac{2}{3}\left(1-\sin^2\theta_T\cos^2\phi_T\right)$
8	$\lvert A_S(0)\rvert\lvert A_\parallel(0)\rvert[\frac{1}{2}(e^{-\Gamma_\mathrm{L}^{(s)}t} - e^{-\Gamma_\mathrm{H}^{(s)}t})\sin(\delta_\parallel-\delta_S)\sin\phi_s \pm e^{-\Gamma_s t}(\cos(\delta_\parallel-\delta_S)\cos(\Delta m_s t) - \sin(\delta_\parallel-\delta_S)\cos\phi_s\sin(\Delta m_s t))]$	$\frac{1}{3}\sqrt{6}\sin\psi_T\sin^2\theta_T\sin 2\phi_T$
9	$\frac{1}{2}\lvert A_S(0)\rvert\lvert A_\perp(0)\rvert\sin(\delta_\perp-\delta_S) \left[(1-\cos\phi_s)\, e^{-\Gamma_\mathrm{L}^{(s)}t} + (1+\cos\phi_s)\, e^{-\Gamma_\mathrm{H}^{(s)}t} \mp 2e^{-\Gamma_s t}\sin(\Delta m_s t)\sin\phi_s\right]$	$\frac{1}{3}\sqrt{6}\sin\psi_T\sin 2\theta_T\cos\phi_T$
10	$\lvert A_0(0)\rvert\lvert A_S(0)\rvert[\frac{1}{2}(e^{-\Gamma_\mathrm{H}^{(s)}t} - e^{-\Gamma_\mathrm{L}^{(s)}t})\sin\delta_S\sin\phi_s \pm e^{-\Gamma_s t}(\cos\delta_S\cos(\Delta m_s t) + \sin\delta_S\cos\phi_s\sin(\Delta m_s t))]$	$\frac{4}{3}\sqrt{3}\cos\psi_T\left(1-\sin^2\theta_T\cos^2\phi_T\right)$

Systematic Uncertainties

2015-2017 Data

	ϕ_s [rad]	$\Delta\Gamma_s$ [ps^{-1}]	Γ_s [ps^{-1}]	$\lvert A_{\parallel}(0)\rvert^2$	$\lvert A_0(0)\rvert^2$	$\lvert A_S(0)\rvert^2$	$\delta_\perp$ [rad]	$\delta_\parallel$ [rad]	$\delta_\perp - \delta_S$ [rad]
Tagging	1.7×10^{-2}	0.4×10^{-3}	0.3×10^{-3}	0.2×10^{-3}	0.2×10^{-3}	2.3×10^{-3}	1.9×10^{-2}	2.2×10^{-2}	2.2×10^{-3}
Acceptance	0.7×10^{-3}	$<10^{-4}$	$<10^{-4}$	0.8×10^{-3}	0.7×10^{-3}	2.4×10^{-3}	3.3×10^{-2}	1.4×10^{-2}	2.6×10^{-3}
ID alignment	0.7×10^{-3}	0.1×10^{-3}	0.5×10^{-3}	$<10^{-4}$	$<10^{-4}$	$<10^{-4}$	1.0×10^{-2}	7.2×10^{-3}	$<10^{-4}$
S–wave phase	0.2×10^{-3}	$<10^{-4}$	$<10^{-4}$	0.3×10^{-3}	$<10^{-4}$	0.3×10^{-3}	1.1×10^{-2}	2.1×10^{-2}	8.3×10^{-3}
Background angles model:									
Choice of fit function	1.8×10^{-3}	0.8×10^{-3}	$<10^{-4}$	1.4×10^{-3}	0.7×10^{-3}	0.2×10^{-3}	8.5×10^{-2}	1.9×10^{-1}	1.8×10^{-3}
Choice of p_T bins	1.3×10^{-3}	0.5×10^{-3}	$<10^{-4}$	0.4×10^{-3}	0.5×10^{-3}	1.2×10^{-3}	1.5×10^{-3}	7.2×10^{-3}	1.0×10^{-3}
Choice of mass interval	0.4×10^{-3}	0.1×10^{-3}	0.1×10^{-3}	0.3×10^{-3}	0.3×10^{-3}	1.3×10^{-3}	4.4×10^{-3}	7.4×10^{-3}	2.3×10^{-3}
Dedicated backgrounds:									
B_d^0	2.3×10^{-3}	1.1×10^{-3}	$<10^{-4}$	0.2×10^{-3}	3.1×10^{-3}	1.4×10^{-3}	1.0×10^{-2}	2.3×10^{-2}	2.1×10^{-3}
Λ_b	1.6×10^{-3}	0.4×10^{-3}	0.2×10^{-3}	0.5×10^{-3}	1.2×10^{-3}	1.8×10^{-3}	1.4×10^{-2}	2.9×10^{-2}	0.8×10^{-3}
Fit model:									
Time res. sig frac	1.4×10^{-3}	1.1×10^{-3}	$<10^{-4}$	0.5×10^{-3}	0.6×10^{-3}	0.6×10^{-3}	1.2×10^{-2}	3.0×10^{-2}	0.4×10^{-3}
Time res. p_T bins	3.3×10^{-3}	1.4×10^{-3}	0.1×10^{-2}	$<10^{-4}$	$<10^{-4}$	0.5×10^{-3}	6.2×10^{-3}	5.2×10^{-3}	1.1×10^{-3}
Total	1.8×10^{-2}	0.2×10^{-2}	0.1×10^{-2}	0.2×10^{-2}	0.4×10^{-2}	0.4×10^{-2}	9.7×10^{-2}	2.0×10^{-1}	0.1×10^{-1}

- Systematics assumed uncorrelated.
- Tagging systematics dominant for ϕ_s; accounting for pile-up dependence, calibration curves model and MC precision, "Punzi" PDFs variations, difference between $B^\pm$ and B_s^0 kinematics.
- Fit-model time resolution systematics dominant for Γ_s and $\Delta\Gamma_s$.

Correlation Table

2015-2017 Data

	$\Delta\Gamma$	Γ_s	$\lvert A_{\|\|}(0)\rvert^2$	$\lvert A_0(0)\rvert^2$	$\lvert A_S(0)\rvert^2$	$\delta_{\|\|}$	$\delta_\perp$	$\delta_\perp - \delta_S$
ϕ_s	−0.111	0.038	0.000	−0.008	−0.015	0.019	−0.001	−0.011
$\Delta\Gamma$	1	−0.563	0.092	0.097	0.042	0.036	0.011	0.009
Γ_s		1	−0.139	−0.040	0.103	−0.105	−0.041	0.016
$\lvert A_{\|\|}(0)\rvert^2$			1	−0.349	−0.216	0.571	0.223	−0.035
$\lvert A_0(0)\rvert^2$				1	0.299	−0.129	−0.056	0.051
$\lvert A_S(0)\rvert^2$					1	−0.408	−0.175	0.164
$\delta_{\|\|}$						1	0.392	−0.041
$\delta_\perp$							1	0.052

Lifetime Uncertainty Plots
(Run1, Run2, [19])

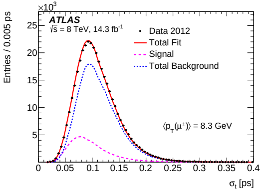

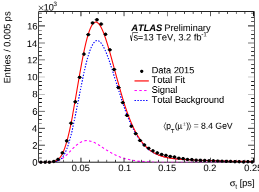

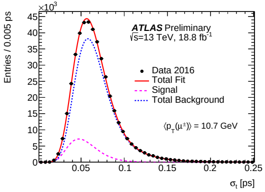

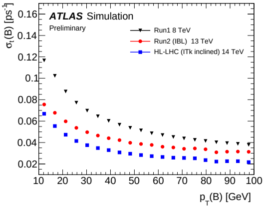

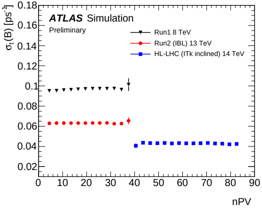

Prospects of CPV Measurements (Upgraded ATLAS, HL-LHC, [20])

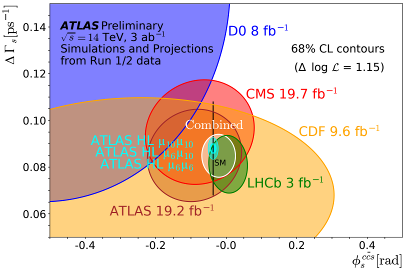

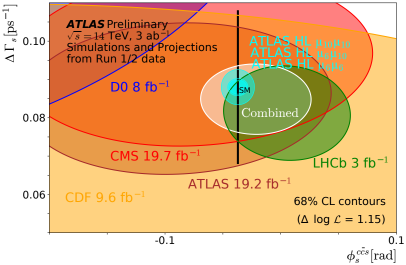

CKM Matrix

Wolfenstein parametrization [21], [22]

$$V_{\text{CKM}} = \begin{pmatrix} 1-\lambda^2/2 & \lambda & A\lambda^3(\rho - i\eta) \\ -\lambda & 1-\lambda^2/2 & A\lambda^2 \\ A\lambda^3(1-\rho-i\eta) & -A\lambda^2 & 1 \end{pmatrix} + \mathcal{O}(\lambda^4), \qquad (8)$$

where the parameters A, ρ, and η are assumed to be of order one.

REFERENCES

References I

[1] M. Kobayashi and T. Maskawa, *CP Violation in the Renormalizable Theory of Weak Interaction*, Prog. Theor. Phys. 49 (1973) 652.

[2] J. Charles *et al.*, *Predictions of selected flavour observables within the Standard Model*, Phys. Rev. D 84 (2011) 033005.

[3] J. Pequenao, *Computer generated image of the whole ATLAS detector*, CERN-GE-0803012.

[4] ATLAS Collaboration, *Invariant mass distributions for oppositely charged muon candidate pairs that pass various triggers, using 2018 data*, https://twiki.cern.ch/twiki/bin/view/AtlasPublic/BPhysicsTriggerPublicResults.

[5] ATLAS Collaboration, *Time-dependent angular analysis of the decay $B_s^0 \to J/\psi\phi$ and extraction of $\Delta\Gamma_s$ and the CP-violating weak phase ϕ_s by ATLAS*, JHEP 1212 (2012) 072.

[6] ATLAS Collaboration, *Flavor tagged time-dependent angular analysis of the $B_s \to J/\psi\phi$ decay and extraction of $\Delta\Gamma$s and the weak phase ϕ_s in ATLAS*, Phys. Rev. D 90 (2014) no.5, 052007.

[7] ATLAS Collaboration, *Measurement of the CP-violating phase ϕ_s and the B_s^0 meson decay width difference with $B_s^0 \to J/\psi\phi$ decays in ATLAS*, JHEP 1608 (2016) 147.

[8] ATLAS Collaboration, *Measurement of the CP violation phase ϕ_s in $B_s \to J/\psi\phi$ decays in ATLAS at 13 TeV*, ATLAS-CONF-2019-009.

[9] CDF Collaboration, *Measurement of the CP-Violating Phase $\beta_s^{J/\psi\phi}$ in $B_s^0 \to J/\psi\phi$ Decays with the CDF II Detector*, Phys. Rev. D 85 (2012) 072002.

[10]

References II

[11] LHCb Collaboration, *Determination of the sign of the decay width difference in the B_s system*, Phys. Rev. Lett. 108 (2012) 241801.

[12] R. Nisius, *On the combination of correlated estimates of a physics observable*, Eur. Phys. J. C 74 (2014) no.8, 3004.

[13] R. Nisius, *BLUE: a software package to combine correlated estimates of physics observables within ROOT using the Best Linear Unbiased Estimate method - Program manual*, Version 1.9.2, http://blue.hepforge.org.

[14] CMS Collaboration, *Measurement of the CP-violating weak phase ϕ_s and the decay width difference $\Delta\Gamma_s$ using the $B_s^0 \to J/\psi\phi(1020)$ decay channel in pp collisions at $\sqrt{s} = 8$ TeV*, Phys. Lett. B 757 (2016) 97.

[15] LHCb Collaboration, *Updated measurement of time-dependent CP-violating observables in $B_s^0 \to J/\psi K^+K^-$ decays*, arXiv:1906.08356 [hep-ex].

[16] F. Dordei, *Precision measurement of the CP-violating phase ϕ_s at LHCb*, LHC seminar, CERN, 7th May 2019, https://indico.cern.ch/event/807907/.

[17] A. Lenz and U. Nierste, *Numerical Updates of Lifetimes and Mixing Parameters of B Mesons*, arXiv:1102.4274 [hep-ph].

[18] Y. Amhis *et al.* (Heavy Flavour Averaging Group), *Averages of b-hadron, c-hadron, and τ-lepton properties as of summer 2016*, Eur. Phys. J. C 77 (2017) no.12, 895 and online update at https://hflav.web.cern.ch.

[19] ATLAS Collaboration, *B_s^0 proper decay time resolution in the $B_s^0 \to J/\psi(\mu^+\mu^-)\phi(K^+K^-)$ decay for Run-1, Run-2 and HL-LHC*, https://atlas.web.cern.ch/Atlas/GROUPS/PHYSICS/PLOTS/BPHYS-2016-001.

[20] ATLAS and CMS Collaborations, *Report on the Physics at the HL-LHC and Perspectives for the HE-LHC*, arXiv:1902.10229 [hep-ex].

References III

[21] L. Wolfenstein, *Parametrization of the Kobayashi-Maskawa Matrix*, Phys. Rev. Lett. 51 (1983) 1945.

[22] A. J. Bevan *et al.*, *The Physics of the B Factories*, Eur. Phys. J. C 74 (2014) 3026.